Check for updates

View Article Online
View Journal

Chemical Science

Accepted Manuscript

This article can be cited before page numbers have been issued, to do this please use: Y. Furukawa, R. Sato, N. FUKAYA, T. Kajitani, T. Katashima and K. Sugiyasu, *Chem. Sci.*, 2026, DOI: 10.1039/D5SC09763K.

This is an Accepted Manuscript, which has been through the Royal Society of Chemistry peer review process and has been accepted for publication.

Accepted Manuscripts are published online shortly after acceptance, before technical editing, formatting and proof reading. Using this free service, authors can make their results available to the community, in citable form, before we publish the edited article. We will replace this Accepted Manuscript with the edited and formatted Advance Article as soon as it is available.

You can find more information about Accepted Manuscripts in the Information for Authors.

Please note that technical editing may introduce minor changes to the text and/or graphics, which may alter content. The journal's standard Terms & Conditions and the Ethical guidelines still apply. In no event shall the Royal Society of Chemistry be held responsible for any errors or omissions in this Accepted Manuscript or any consequences arising from the use of any information it contains.

ROYAL SOCIETY OF CHEMISTRY

rsc.li/chemical-science

Please do not adjust margins

View Article Online
DOI: 10.1039/D5SC09763K

ARTICLE

Linear and branched supramolecular polymers formed from isomeric monomers as revealed by solution viscoelasticity

Received 00th January 20xx,
Accepted 00th January 20xx

DOI: 10.1039/x0xx00000x

Yufuka Furukawa,[a]† Ren Sato,[b]† Natsumi Fukaya,[a] Takashi Kajitani,[c] Takuya Katashima*[b] and Kazunori Sugiyasu*[a]

Supramolecular polymers (SPs) assembled through non-covalent interactions provide a promising platform for designing soft materials with dynamic and tunable properties. However, the viscoelastic properties of their solutions remain poorly understood, largely due to the tendency of SP chains to bundle into thick supramolecular fibers, often resulting in precipitation or gelation. In this study, we show that bundle formation can be effectively suppressed by appropriate design of the surface of SPs through alteration of their side chains. Structural analyses revealed that the resulting SPs are homogeneously solvated, permitting their rheological characterization. Notably, we found that even subtle modifications, such as positional isomerism of the side chains, can dramatically alter the physical properties of SP solutions. Our findings, therefore, highlight the critical role of side chains in governing hierarchical structures and macroscopic properties of SPs, offering a design strategy for engineering functional supramolecular materials.

Introduction

A discotic molecule equipped with properly designed hydrogen bonding sites at its periphery can undergo spontaneous self-assembly to form a one-dimensional (1D) columnar polymeric array, thereby forming a supramolecular polymer (SP) chain.[1] Supramolecular polymerization of such monomers is well understood on the basis of a nucleation–elongation mechanism.[2] In addition, under kinetic control, living supramolecular polymerization is possible, which permits precise control of the polymer chain length[3] and the creation of block architectures.[4] As such, SPs can nowadays be rationally designed from the monomer level. However, at the polymer level, the design principles that govern the behavior of SP chains in solution, particularly with respect to their viscoelastic properties, remain poorly understood.[2,5-11,‡]

One difficulty in investigating the solution viscoelasticity of SPs lies in their propensity to bundle into thick 1D fibers, rather than to exist as individually solvated polymeric chains (Fig. 1a). This bundling behavior is probably associated with a polymerization mechanism that resembles the crystallization of a small molecule, i.e., a nucleation–elongation process. Consequently, SPs in solution often form precipitates or colloidal dispersions that take the form of physical gels, commonly referred to as low-molecular-weight gels (LMWGs).[12] Rheological studies of LMWGs have been extensively conducted

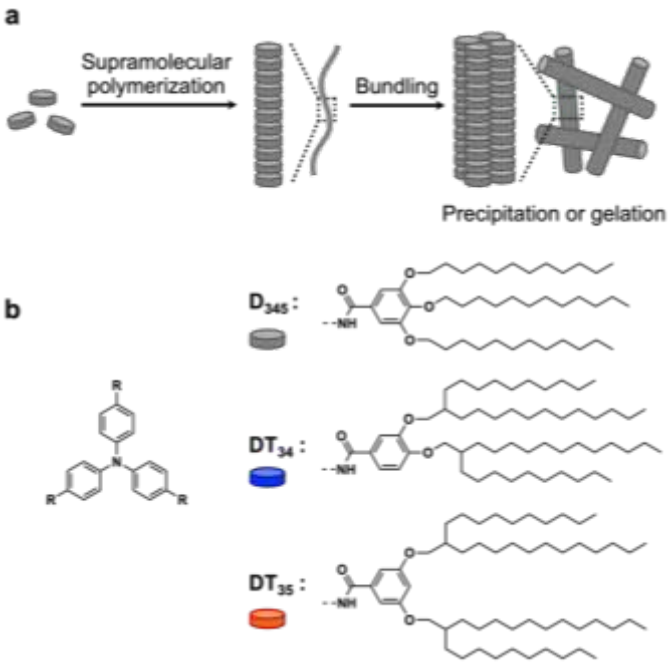

Fig. 1 (a) Schematic representation of supramolecular polymerization that accompanies bundling. (b) Chemical structures of the triphenylamine-based monomers. **D_{345}** contains linear dodecyl chains. **DT_{34}** and **DT_{35}** have 2-decyltetradecyl chains (as a racemic mixture) at different positions of the peripheral phenyl groups.

[a] Department of Polymer Chemistry, Graduate School of Engineering, Kyoto University, Kyotodaigaku-katsura, Saikyo-ku, Kyoto 615-8510, Japan. E-mail: sugiyasu.kazunori.8z@kyoto-u.ac.jp
[b] Department of Bioengineering, Graduate School of Engineering, The University of Tokyo, 7-3-1 Hongo, Bunkyo-ku, Tokyo 113-8656, Japan. E-mail: katashima@g.ecc.u-tokyo.ac.jp
[c] Core Facility Center, Research Infrastructure Management Center, Institute of Science Tokyo, 4259 Nagatsuta, Midori-ku, Yokohama 226-8501, Japan.
† Y.F. and R.S. contributed equally.
§ Electronic Supplementary Information (ESI) available: See DOI: 10.1039/x0xx00000x

Open Access Article. Published on 14 April 2026. Downloaded on 4/15/2026 3:10:24 AM.
This article is licensed under a Creative Commons Attribution-NonCommercial 3.0 Unported Licence.

Chemical Science Accepted Manuscript

View Article Online
DOI: 10.1039/D5SC09763K

Open Access Article. Published on 14 April 2026. Downloaded on 4/15/2026 3:10:24 AM.
This article is licensed under a Creative Commons Attribution-NonCommercial 3.0 Unported Licence.

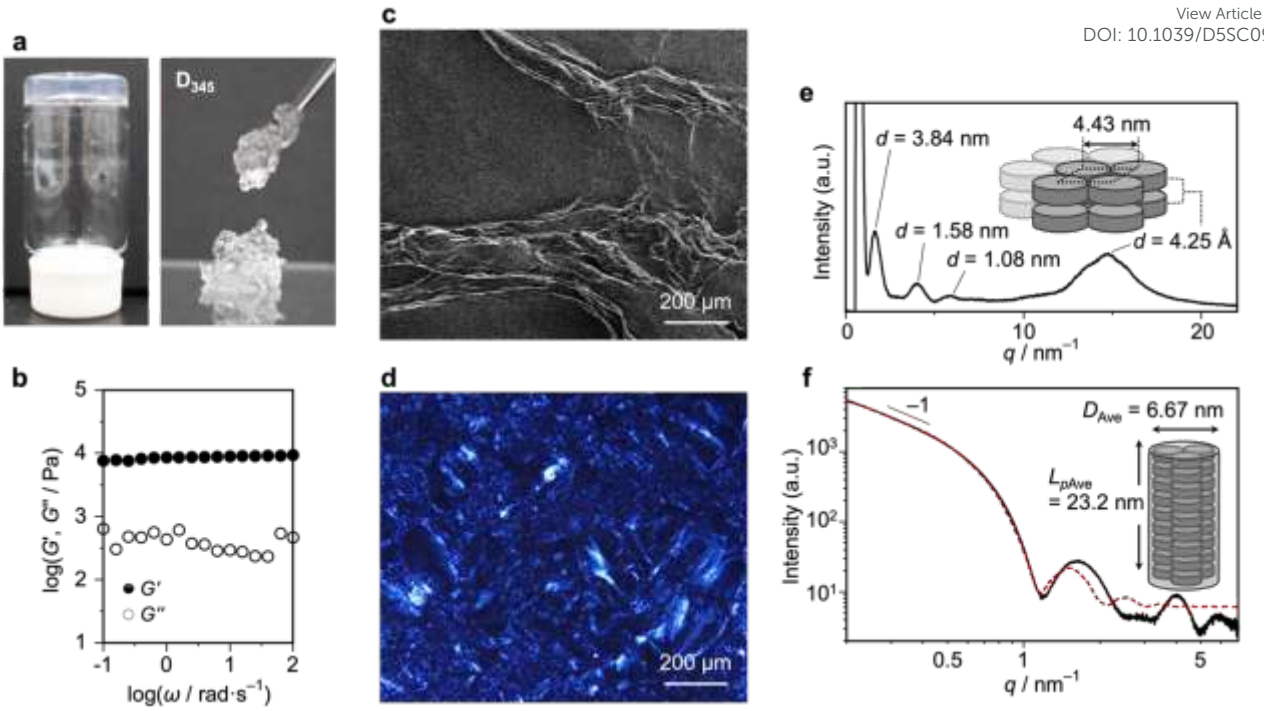

Fig. 2 (a) Photograph of a dodecane gel of $\mathbf{D_{345}}$ at a concentration of 10 mM. (b) Angular frequency dependence of the storage (*G'*, filled circle) and loss (*G''*, hollow circle) moduli of $\mathbf{D_{345}}$ at a concentration of 10 mM in dodecane. (c) SEM images of a dried sample prepared from $\mathbf{D_{345}}$ gel. (d) POM image of $\mathbf{D_{345}}$ gel at 10 mM. (e) WAXS and (f) SAXS profiles of a 10 mM solution of $\mathbf{D_{345}}$ in dodecane. The fitting curve (red dashed line) was obtained on the basis of a cylinder model.

to assess their mechanical stability[13] and to determine critical gelation parameters, including the gelation temperature,[14] concentration,[15] and time.[16] Although LMWGs hold promise for a wide range of applications,[12,17] their inherent bundling and gelation phenomena significantly impede the investigation of SP chains within the framework of conventional polymer physics.

Tuning the solvent polarity based on solubility parameters would prevent SP chains from bundling.[18] As an alternative strategy, we recently demonstrated that bundling of SPs can be effectively suppressed by an appropriate design of the surface of the SP chain.[19] Specifically, by introducing a degree of randomness into the lengths of the alkyl side chains covering the SP surface, we were able to obtain a homogeneous solution of individually separated SP chains, without gelation, even at relatively high concentrations (~ mM). This, in turn, permitted solution spinning of the resulting SP. We anticipated that this strategy might allow us to study the solution viscoelasticity of SPs. To expand our molecular-design concept, we employed a branched alkyl chain. Branched alkyl groups have previously been used as side chains to improve the solubilities of rigid π-conjugated polymers.[20] Moreover, branched alkyl chains have been used as "entropic ligands" on nanocrystal surfaces, where the ligands harvest conformational entropy in solution and disrupt the crystalline interdigitation typically observed with linear alkyl chains, thereby enhancing the colloidal solubility.[21] We hoped that incorporating such side chains onto the surface of SPs might similarly suppress the bundling of the SP chains.

In this study, we designed three monomers based on triphenylamine with distinct alkyl side chains:[22-23] $\mathbf{D_{345}}$, which carries linear dodecyl (**D**) chains, and $\mathbf{DT_{34}}$ and $\mathbf{DT_{35}}$, which carry branched 2-decyltetradecyl (**DT**) chains (Fig. 1b). The numerical subscripts indicate the positions of the alkyl chains on the benzamide groups. Whereas the SPs derived from $\mathbf{D_{345}}$ showed heavy bundling and formed an LMWG, those consisting of $\mathbf{DT_{34}}$ and $\mathbf{DT_{35}}$ were homogeneously soluble in aliphatic solvents. Although common characterization techniques for SPs—such as variable-temperature absorption spectroscopy, atomic force microscopy, and X-ray scattering—could not clearly distinguish the SPs formed from $\mathbf{DT_{34}}$ and $\mathbf{DT_{35}}$, the flow dynamics of these solutions showed marked differences. Rheological investigations revealed that whereas the SP from $\mathbf{DT_{34}}$ showed a similar behavior to a "linear" covalent polymer in exhibiting reptation-driven relaxation, the SP from $\mathbf{DT_{35}}$ showed "branched" covalent polymer-like dynamics, dominated by arm retraction. These findings demonstrate that engineering the surface of SPs—even by such subtle modifications as positional isomerism of the side chains—can dramatically influence the physical properties of SP chains.

Results

Characterization of $\mathbf{D_{345}}$ gel

We first investigated the supramolecular polymerization of $\mathbf{D_{345}}$ as a reference monomer bearing commonly used linear alkyl chains (i.e., dodecyl chains). $\mathbf{D_{345}}$ was dissolved in hot dodecane to form a 10 mM solution, and the solution was

Chemical Science Accepted Manuscript

 This journal is © The Royal Society of Chemistry 20xx

View Article Online
DOI: 10.1039/D5SC00767K

Open Access Article. Published on 14 April 2026. Downloaded on 4/15/2026 3:10:24 AM.
This article is licensed under a Creative Commons Attribution-NonCommercial 3.0 Unported Licence.

subsequently cooled to ambient temperature. As observed for other discotic monomers,[24] **D$_{345}$** formed an LMWG (Fig. 2a; left). Complementary oscillatory rheology measurements revealed that the storage modulus (G') exceeded the loss modulus (G'') across the entire frequency range examined (0.1–100 rad s^{-1}), confirming the solid-like nature of this material (Fig. 2b). However, as often observed for LMWGs, the gel formed by **D$_{345}$** was mechanically fragile and, upon the application of a mechanical stress, it readily collapsed and released the solvent (Fig. 2a; right).

Scanning electron microscopy (SEM) of the dried gel revealed the formation of thick supramolecular fibers composed of bundled SPs (Fig. 2c). Polarized optical microscopy (POM) images of the gel exhibited birefringence at the microscopic scale, indicating the presence of large crystalline aggregates (Fig. 2d). Under diluted conditions (~ 5.0 × 10^{-5} M), the supramolecular polymers of **D$_{345}$** precipitated, most likely due to their crystalline nature [Supplementary Information (SI); Fig. S1]. To further characterize the structure of the supramolecular fibers in the gel state, wide-angle X-ray scattering (WAXS) and small-angle X-ray scattering (SAXS) measurements were performed. The WAXS profile of the **D$_{345}$** gel showed scattering peaks at q = 1.67 (d = 3.84 nm), 4.08 (d = 1.58 nm), and 5.83 nm^{-1} (d = 1.08 nm) (Fig. 2e). The ratio of these q values approximates to 1:√7:√12, which is consistent with a hexagonal packing of the SPs with a calculated diameter of 4.43 nm (the diameter of **D$_{345}$** estimated from molecular model is 5.0 nm (Fig. S3a)). A peak at q = 14.71 nm^{-1} (d = 4.25 Å) was attributed to the distance between nitrogen centers of the stacked triphenylamine units, in agreement with previous reports.[22] The stacking appeared to be stabilized by intermolecular hydrogen bonding of the amide groups, as suggested by the observation of a N–H stretching vibration at 3265 cm^{-1} in the FT-IR spectrum (SI; Fig. S2). The SAXS profile of **D$_{345}$** exhibited a slope of –1 in the low-q region, characteristic of a cylindrical structure (Fig. 2f).[25] A cylindrical model fitted to the SAXS data yielded an average diameter (D_{Ave}) of 6.67 nm and an average persistence length (L_{pAve}) of 23.2 nm (SI; Table S1). Collectively, these results show that the SPs of **D$_{345}$**, which are covered with linear dodecyl chains, are prone to bundle into thick supramolecular fibers, thereby forming an organogel.

Characterization of SPs of DT$_{34}$ and DT$_{35}$

The **D$_{345}$** gel retained its shape for over a month without flowing (Fig. 3e). In sharp contrast to this observation, solutions of both **DT$_{34}$** and **DT$_{35}$** (10 mM in dodecane) did not undergo gelation and remained in a fluid state (Figs. 3a–d). At first glance, a noticeable difference was observed in the viscosities of these solutions (discussed later). POM observations revealed no evidence of the presence of large aggregates (SI; Fig. S4), suggesting that SP chains of **DT$_{34}$** and **DT$_{35}$** remained well dispersed in the solutions.

The WAXS patterns of the solutions showed a reflection at q = 14.52 nm^{-1} (d = 4.34 Å) for **DT$_{34}$** and at q = 14.52 nm^{-1} (d = 4.32 Å) for **DT$_{35}$**, corresponding to the N–N stacking distance (Fig. 4b). In addition, FT-IR spectra of **DT$_{34}$** and **DT$_{35}$** showed a N–H stretching band at 3304 cm^{-1} and 3300 cm^{-1}, confirming the formation of intermolecular hydrogen bonds (SI; Fig. S5). These results suggest that both **DT$_{34}$** and **DT$_{35}$** form 1D polymeric arrays, as was the case for **D$_{345}$**. In fact, the SAXS profiles of 10 mM solutions of these two SPs exhibited a slope of –1 in the low-q region (q < 0.5 nm^{-1}), indicative of cylindrical structures (Fig. 4c). Importantly, the SAXS data fitted to a cylindrical model gave L_{pAve} = 17.7 nm and D_{Ave} = 2.81 nm for **DT$_{34}$** and L_{pAve} = 16.9 nm and D_{Ave} = 2.65 nm for **DT$_{35}$** (SI; Table S1). The diameters of the SPs formed from **DT$_{34}$** and **DT$_{35}$**, therefore, matched the dimensions of the aromatic cores in the monomers (Figs. 4a and SI; S3b), indicating that these SPs exist

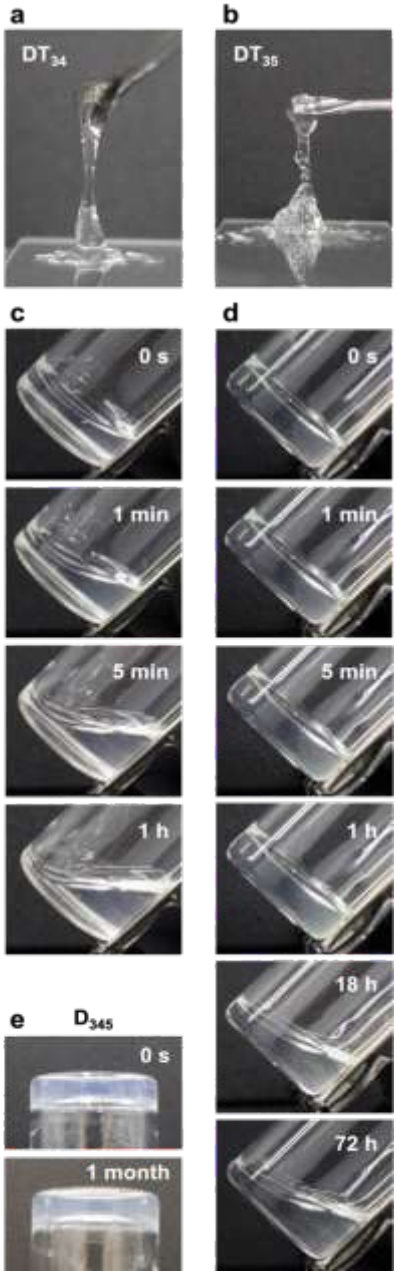

Fig. 3 Photographs of 10 mM dodecane solutions of SPs consisting of (a) **DT$_{34}$** and (b) **DT$_{35}$**, and of vial-tilt tests of the solutions of (c) **DT$_{34}$** and (d) **DT$_{35}$**. (e) Time-lapse images of a vial-inversion test of a dodecane gel of **D$_{345}$** at a concentration of 10 mM.

Chemical Science Accepted Manuscript

View Article Online DOI: 10.1039/D5SC07637H

as individually solvated chains in solution without bundling. In fact, unlike the case of **D$_{345}$** (Fig. 2e), no crystalline diffraction peaks attributable to the hexagonal packing of the SP chains were observed in the WAXS profiles of the SPs (Fig. 4b). The longer L_{pAve} of **D$_{345}$** compared to those of **DT$_{34}$** and **DT$_{35}$** is consistent with the bundled, and thus stiff supramolecular fibers consisting of **D$_{345}$**. Figs. 4d and 4e show atomic-force microscopy (AFM) images of the SP chains. We surmise that the observed network-like structures were formed during the sample preparation process, specifically, during spin-coating onto the silicon wafer. Importantly, the SPs of both **DT$_{34}$** and **DT$_{35}$** had average heights of approximately 2.5 nm (Figs. 4d and 4e, bottom, and SI; S6), which is in good agreement with the SAXS analysis. These results suggest that the introduction of the 2-decyltetradecyl group effectively prevents the SP chains from bundling, and that the position of the alkyl chain has a minimal impact on the primary structure of the SP.

To elucidate the supramolecular polymerization mechanism, variable-temperature absorption spectral measurements were conducted for solutions of **DT$_{34}$** and **DT$_{35}$** at various concentrations (3.0×10^{-5} to 20×10^{-5} M: SI; Figs. S7 and S8). The dissociation curves of **DT$_{34}$** and **DT$_{35}$** were analyzed based on an equilibrium (EQ) model[26] (Figs. 4f and 4g) and the van't Hoff plots[27] (SI; Figs. S9–S11). The fitting details are described in the SI, and the resulting thermodynamic parameters are summarized in Tables S2 and S4. In brief, the supramolecular polymerizations of both **DT$_{34}$** and **DT$_{35}$** were characterized by stronger gains in elongation enthalpy (ΔH_e = –191.1 and –155.9 kJ/mol, respectively) compared with typical benzene-1,3,5-tricarboxamide (BTA)-based SPs (ΔH_e = –60.1 kJ/mol in heptane),[27b] suggesting that the SPs of **DT$_{34}$** and **DT$_{35}$** form through relatively strong monomer–monomer interactions associated with the larger core. The changes in the Gibbs free energy (ΔG_e) at 298 K, determined from the EQ model, were –34.4 kJ/mol for **DT$_{34}$** and –35.2 kJ/mol for **DT$_{35}$** (SI; Table S2). The

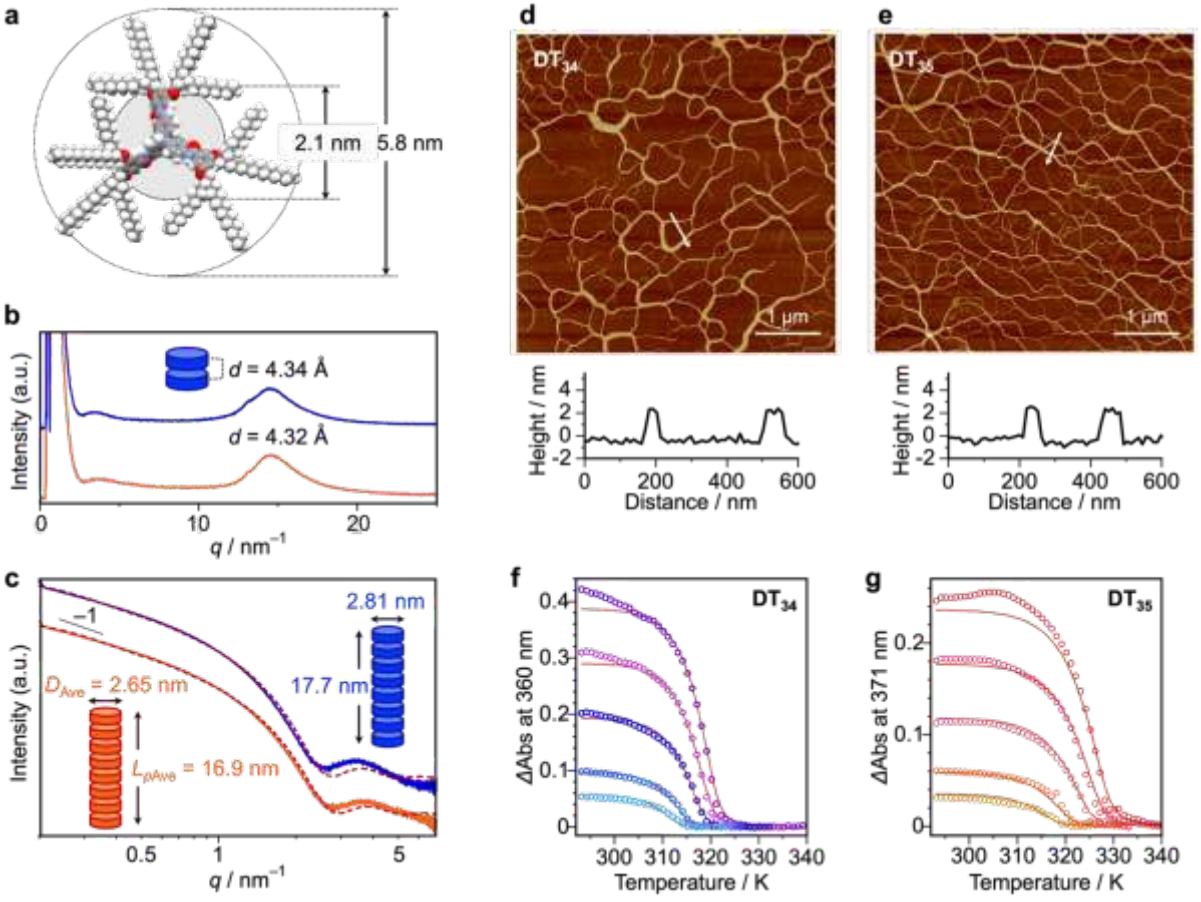

Fig. 4 (a) Molecular model of **DT$_{35}$**. (b) WAXS and (c) SAXS profiles of 10 mM dodecane solutions of **DT$_{34}$** (blue) and **DT$_{35}$** (orange). The fitting curves (red dashed line) were obtained from a cylinder model. (d, e) AFM height images of SPs consisting of (d) **DT$_{34}$** (e) and **DT$_{35}$**, spin-coated from dodecane solutions (5.0×10^{-5} M) onto silicon wafers. Cross-sectional analyses along the white arrows are shown below the corresponding AFM images. (f, g) Changes in the absorbance as a function of temperature for (f) **DT$_{34}$** and (g) **DT$_{35}$** at various concentrations: [**DT$_{34}$** or **DT$_{35}$**] = 3.0×10^{-5}, 5.0×10^{-5}, 10.0×10^{-5}, 15.0×10^{-5}, or 20.0×10^{-5} M. Fitting curves are shown as red lines.

Open Access Article. Published on 14 April 2026. Downloaded on 4/15/2026 3:10:24 AM. This article is licensed under a Creative Commons Attribution-NonCommercial 3.0 Unported Licence.

Chemical Science Accepted Manuscript

This journal is © The Royal Society of Chemistry 20xx

View Article Online
DOI: 10.1039/D5SC09763K

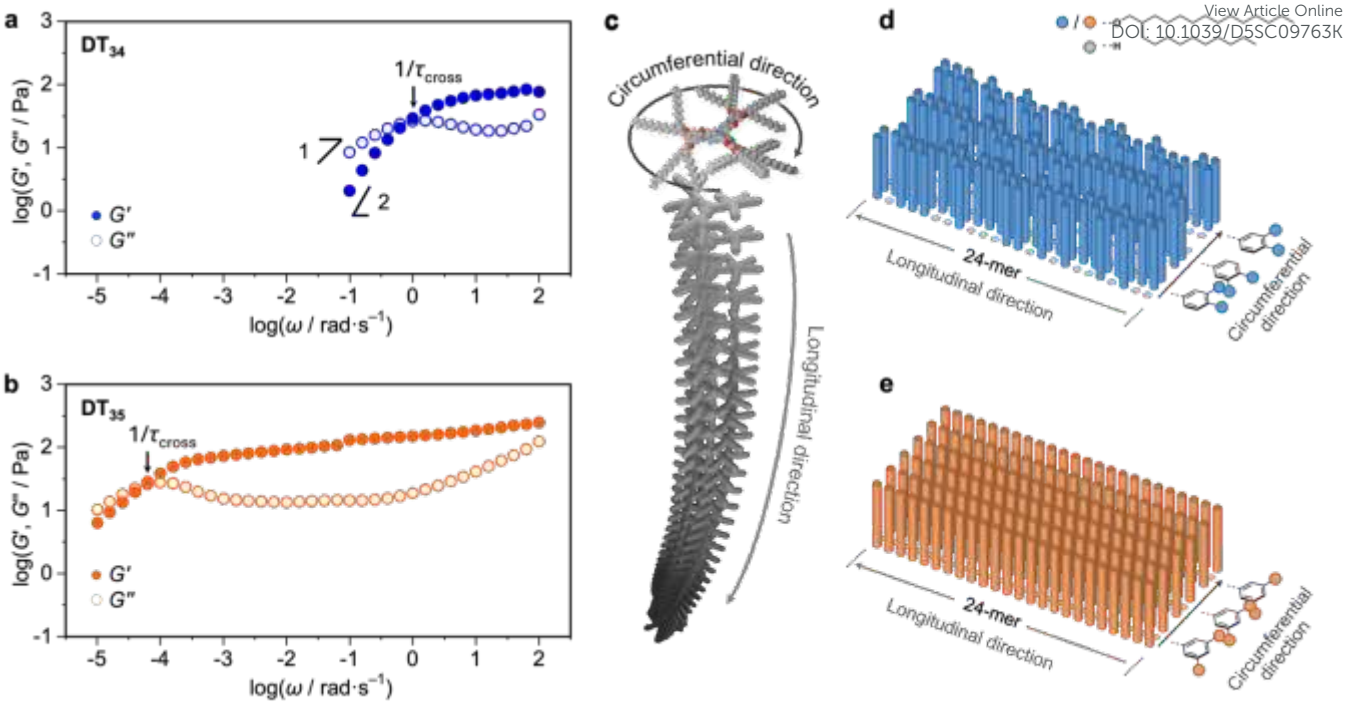

Fig. 5 Angular frequency dependence of the storage (G', filled circle) and loss (G'', hollow circle) moduli for (a) **DT$_{34}$** and (b) **DT$_{35}$** at a concentration of 10 mM. (c) Schematic representation of a supramolecular polymer. Flattened views of the surface of the supramolecular polymers of (d) **DT$_{34}$** and (e) **DT$_{35}$**. The surfaces are shown in 2D, by unwrapping the supramolecular polymers longitudinally. The graphs show the positions of the 2-decyltetradecyl groups along the supramolecular polymer chains, each consisting of 24 monomers. Both **DT$_{34}$** and **DT$_{35}$** have six 2-decyltetradecyl groups surrounding the surface of the supramolecular polymer. In the case of **DT$_{34}$** (d), rotational conformers, which are assumed to be randomly distributed along the polymer chain, generate the rough surface.

van't Hoff plots provided a consistent ΔG_e values (SI; Table S4). Given the lack of substantial difference in the ΔG_e values of **DT$_{34}$** and **DT$_{35}$**, we infer that positional isomerism of the alkyl chains exerts a minimal influence on the monomer–monomer interactions. We were unable to determine the thermodynamic parameters for **D$_{345}$** because of the precipitation (see above).

Viscoelastic behaviors of SPs of DT$_{34}$ and DT$_{35}$

The introduction of 2-decyltetradecyl groups as side chains suppressed the bundling of SPs and the gelation; consequently, homogeneous solutions of individually solvated SPs were obtained, which permitted their investigation within the framework of conventional polymer physics. Fig. 5 shows the angular frequency (ω) dependences of the storage modulus (G') and loss modulus (G'') of the dodecane solutions of **DT$_{34}$** and **DT$_{35}$**. The crossover points between G' and G'' are clearly observable, marking a transition from elastic to viscous behavior, and indicating the onset of a terminal relaxation regime. Our analysis began with an examination of the similarities between the two systems (Figs. 5a and 5b). In both **DT$_{34}$** and **DT$_{35}$**, the value of G' leveled off at higher frequencies, known as the rubbery plateau; this typically arises from entanglements of sufficiently long polymer chains.

We investigated the concentration dependence of the plateau modulus (G_p), defined as the value of G' at the minimum of tan δ (SI; Figs. S12 and S13), in the range of 5–10 mM, where sufficient torque was obtained across the rubbery plateau. The G_p values for **DT$_{34}$** and **DT$_{35}$** were comparable and increased with concentration, following the power-law relationship $G_p \sim c^{1.5}$. According to well-established experimental and theoretical studies on entangled covalent polymers, G_p is primarily governed by the density of entanglements and, consequently, exhibits a concentration dependence described by the relationship $G_p \sim c^{\alpha}$. Here, the value of α depends on the flexibility of the polymer chain. For instance, the value of α for a flexible polymer has been reported to be 2,[28] reflecting the probability of the two-body contacts required to form an entanglement point.[29] When the flexibility decreases, and the persistence length becomes comparable to the contour length (referred to as a semi-flexible polymer), entanglement is suppressed. Accordingly, the concentration dependence follows a weaker power-law relationship, with α reported to be 1.5.[30] The concentration dependence of G_p observed for both **DT$_{34}$** and **DT$_{35}$** ($G_p \sim c^{1.5}$, see above) suggests that these SPs can, therefore, be classified as semi-flexible polymers.

All the results described above indicated that the SPs consisting of **DT$_{34}$** and **DT$_{35}$** are similar in terms of their structures and stabilities. However, the flow properties of the SPs of **DT$_{34}$** and **DT$_{35}$** differed markedly (Figs. 3c and 3d), suggesting that there are distinct underlying mechanisms governing their macroscopic behavior. We therefore

Open Access Article. Published on 14 April 2026. Downloaded on 4/15/2026 3:10:24 AM.
This article is licensed under a Creative Commons Attribution-NonCommercial 3.0 Unported Licence.
Chemical Science Accepted Manuscript

View Article Online DOI: 10.1039/D5SC00767K

subsequently directed our attention to the behavior of these SPs in the lower-frequency regime.

In the case of **DT$_{34}$**, a power-law dependence ($G' \sim \omega^1$, $G'' \sim \omega^2$ as indicated in Fig. 5a) was observed immediately after the rubbery plateau, toward the terminal relaxation regime; this is a characteristic of an entangled "linear" covalent polymer (see, TOC figure).[31] That is, the SP chains do not pass through one another, and the chain motion is constrained in the 1D direction along the polymer backbone: a so-called reptation mode. This reptation mode relaxes stress while progressively disentangling the SP chains. The relaxation time can be estimated as the reciprocal of the frequency at the crossover point (τ_{cross}); for the SPs of **DT$_{34}$**, the τ_{cross} value was approximately 1 sec.

In contrast, both G' and G'' of **DT$_{35}$** gradually approached a power-law dependence toward the terminal relaxation regime, without a pronounced maximum in G''. That is, the relaxation dynamics were characterized by a broad and continuous spectrum extending from the high-frequency domain to the terminal relaxation regime. This characteristic resembles the relaxation of entangled "branched" covalent polymers (Fig. 5d).[28b,32] The branch points immobilize chain segments, and the reptation mode is no longer dominant in the relaxation mechanism. Consequently, stress relaxation occurs instead through arm retraction, a process in which a polymer chain withdraws along its own contour toward the branch point. As such, the observed broad spectrum of values of G'' is attributable to the variety of time scales associated with localized motions, including arm retraction. Notably, τ_{cross} of the SPs consisting of **DT$_{35}$** was approximately 2×10^4 sec, representing a value that is four orders of magnitude greater than that for **DT$_{34}$**.

Discussion

Despite the recent developments in the mechanistic understanding of supramolecular polymerization mechanisms, the design principles that govern the behavior of SP chains in solution, particularly with respect to their viscoelastic properties, remain poorly understood. In this study, we focused on the side-chain structures of SPs. The reference monomer **D$_{345}$**, bearing the commonly used linear dodecyl chains, formed SPs that bundled into thick supramolecular fibers, which, as expected, led to gelation of solutions at concentrations above 1 mM. In contrast, the newly designed **DT$_{34}$** and **DT$_{35}$**, possessing branched racemic 2-decyltetradecyl chains, gave homogeneous solutions containing well-solvated SPs, even at higher concentrations of the order of 10 mM. Common characterization techniques such as SAXS, AFM, and temperature-dependent absorption spectroscopy were unable to distinguish the SPs of **DT$_{34}$** and **DT$_{35}$**. Intriguingly, however, the flow properties of these SPs differed markedly, and rheological analyses provided the following insights.

(1) Both **DT$_{34}$**- and **DT$_{35}$**-based SPs behave like covalent polymers in that their chain scission and recombination processes are too slow to contribute to stress relaxation. This behavior contrasts with the dynamics of "living" polymers[33] and the "phantom-crossing"[9] mechanisms proposed by Cates and Shikata, respectively, to explain the terminal relaxation dynamics of wormlike micelles and certain supramolecular polymers (such as that of BTA).[9,10] In these previously investigated systems, the lifetime of the main chain was shorter than the global chain dynamics (reptation time), permitting chain breakage and recombination (or crossing) events to govern the terminal relaxation. In this context, it is noteworthy that Van Zee and co-workers recently demonstrated, through passive microrheological measurements, that biphenyltetracarboxamide (BPTA)-based SPs also exhibit a covalent polymer-like behavior.[11] Such "non-living" SPs remain rare, and the ability to control their relaxation modes by molecular design might open new avenues for SP-based materials. To this end, in addition to controlling monomer–monomer interactions (i.e., ΔH_e), a strategic control of SP–SP interactions could play a key role in material design, as exemplified by the contrasting behaviour of **D$_{345}$**.

(2) The subtle structural difference between **DT$_{34}$** and **DT$_{35}$** led to significant variations in their solution viscoelastic behavior. Rheological characterization suggested that SPs formed from **DT$_{35}$** contain branching points. Given the 1D columnar structure of the SP, these branching points are probably formed through *lateral* interaction between two SP chains. Note that the alkyl chains of **DT$_{35}$** are symmetrically substituted with respect to the amide bond, and, as such, should produce a relatively uniform SP surface (Fig. 5e). We infer that, although not as prominent as **D$_{345}$**, such surface uniformity facilitates SP–SP interactions, thereby promoting the formation of a branching point. In contrast, the alkyl chains of **DT$_{34}$** are asymmetrically substituted relative to the amide bond at 3,4-positions. This asymmetry introduces conformational diversity of the alkyl chains through rotation of the benzamide group, which is distributed randomly at the periphery of **DT$_{34}$** monomer,[19] thereby leading to a disordered SP surface (Fig. 5d). We surmise that such surface disorder suppresses SP–SP interactions, yielding a situation distinct from that observed for **DT$_{35}$**.

Conclusions

As a step toward advancing this research field by molecular-level understanding, our findings highlight the critical role of side chains in tuning the hierarchical assembly and macroscopic properties of SPs. We believe that controlling SP–SP interactions by molecular design might permit precise and engineering and processing of SP-based functional soft materials.[19]

Author contributions

Open Access Article. Published on 14 April 2026. Downloaded on 4/15/2026 3:10:24 AM. This article is licensed under a Creative Commons Attribution-NonCommercial 3.0 Unported Licence.

Chemical Science Accepted Manuscript

This journal is © The Royal Society of Chemistry 20xx

View Article Online
DOI: 10.1039/D5SC09763K

K.S. conceived the project. Y.F. synthesized the monomers, characterized their supramolecular polymerization, and prepared solutions of supramolecular polymers. R.S. conducted viscoelastic measurements. Y.F. and R.S. contributed equally. T.K.[c] conducted WAXS and SAXS measurements. All authors discussed the results. N.F., T.K.[b] and K.S. wrote the paper with input from all the authors.

Conflicts of interest

There are no conflicts to declare.

Data availability

The data supporting this study are provided in the ESI.§

Acknowledgements

The work is supported by the Japan Society for the Promotion of Science (JSPS) KAKENHI grant no. JP25K18071 (N.F), no. JP22H02134 (K.S); no. JP23K17941 (K.S.); no. JP24H01712 (K.S.), in a Grant-in-Aid Scientific Research for Transformative Research Areas (A) "Materials Science of Meso-Hierarchy"; and by Japan Science and Technology Agency (JST) grant no. JPMJCR23L2 (K.S., T.K.[b] & T.K.[c]) in Precise Material Science for Degradation and Stability, CREST. K.S. acknowledges financial support from The Murata Science Foundation, Sekisui Chemical Grant Program, The Mitsubishi Foundation, Masuyakinen Basic Research Foundation, Fujimori Science and Technology Foundation, and The Samco Foundation. We are grateful to Prof. Kazuo Tanaka (Kyoto University) and Assist. Prof. Masayuki Gon (Kyoto University) for use of the sputter coater for SEM measurements.

Notes and references

‡ It should be noted that there is another class of SPs, formed from ditopic monomers.[1,5] These monomers self-assemble through host-guest complexation[6], complementary hydrogen bonding,[7] or metal-ligand interaction[8] and their polymerization process follows an isodesmic model.[2] In principle, supramolecular polymerization of this type cannot be controlled kinetically. The viscoelastic properties of these polymers in solution have been extensively studied, owing to their homogeneous solubility in water[8] and organic solvents.[6,7] As such, this class of SPs differs from those examined in the present study and is not discussed in the context of this manuscript.

1 L. Brunsveld, B. J. B. Folmer, E. W. Meijer and R. P. Sijbesma, Supramolecular Polymers, *Chem. Rev.*, 2001, **101**, 4071–4098.
2 T. F. A. De Greef, M. M. J. Smulders, M. Wolffs, A. P. H. J. Schenning, R. P. Sijbesma and E. W. Meijer, Supramolecular Polymerization, *Chem. Rev.*, 2009, **109**, 5687–5754.
3 (a) S. Ogi, K. Sugiyasu, S. Manna, S. Samitsu and M. Takeuchi, Living supramolecular polymerization realized through a biomimetic approach, *Nat. Chem.*, 2014, **6**, 188–195; (b) J. Kang, D. Miyajima, T. Mori, Y. Inoue, Y. Itoh and T. Aida, A rational strategy for the realization of chain-growth supramolecular polymerization, *Science*, 2015, **347**, 646–651; (c) S. Ogi, V. Stepanenko, K. Sugiyasu, M. Takeuchi and F. Würthner, Mechanism of Self-Assembly Process and Seeded Supramolecular Polymerization of Perylene Bisimide Organogelator, *J. Am. Chem. Soc.*, 2015, **137**, 3300–3307; (d) M. Wehner and F. Würthner, Supramolecular polymerization through kinetic pathway control and living chain growth, *Nat. Rev. Chem.*, 2020, **4**, 38–53; (e) K. Sugiyasu, A case study of monomer design for controlled/living supramolecular polymerization, *Polym. J.*, 2021, **53**, 865–875.
4 (a) S. H. Jung, D. Bochicchio, G. M. Pavan, M. Takeuchi and K. Sugiyasu, A Block Supramolecular Polymer and Its Kinetically Enhanced Stability, *J. Am. Chem. Soc.*, 2018, **140**, 10570–10577; (b) W. Wagner, M. Wehner, V. Stepanenko and F. Würthner, Supramolecular Block Copolymers by Seeded Living Polymerization of Perylene Bisimides, *J. Am. Chem. Soc.*, 2019, **141**, 12044–12054; (c) A. Sarkar, R. Sasmal, C. Empereur-mot, D. Bochicchio, S. V. K. Kompella, K. Sharma, S. Dhiman, B. Sundaram, S. S. Agasti, G. M. Pavan and S. J. George, Self-Sorted, Random, and Block Supramolecular Copolymers via Sequence Controlled, Multicomponent Self-Assembly, *J. Am. Chem. Soc.*, 2020, **142**, 7606–7617; (d) N. Sasaki, J. Kikkawa, Y. Ishii, T. Uchihashi, H. Imamura, M. Takeuchi and K. Sugiyasu, Multistep, site-selective noncovalent synthesis of two-dimensional block supramolecular polymers, *Nat. Chem.*, 2023, **15**, 922–929.
5 T. Haino, Molecular-recognition-directed formation of supramolecular polymers, *Polym. J.*, 2013, **45**, 363–383.
6 (a) R. K. Castellano, R. Clark, S. L. Craig, C. Nuckolls and J. Rebek, Emergent mechanical properties of self-assembled polymeric capsules, *Proc. Natl. Acad. Sci. USA.*, 2000, **97**, 12418–12421; (b) T. Haino, A. Watanabe, T. Hirao and T. Ikeda, Supramolecular Polymerization Triggered by Molecular Recognition between Bisporphyrin and Trinitrofluorenone, *Angew. Chem. Int. Ed.*, 2012, **51**, 1473–1476; (c) B. Zheng, F. Wang, S. Dong and F. Huang, Supramolecular polymers constructed by crown ether-based molecular recognition, *Chem. Soc. Rev.*, 2012, **41**, 1621–1636; (d) D. Xia and M. Xue, A supramolecular polymer gel with dual-responsiveness constructed by crown ether based molecular recognition, *Polym. Chem.*, 2014, **5**, 5591–5597; (e) L. Wang, L. Cheng, G. Li, K. Liu, Z. Zhang, P. Li, S. Dong, W. Yu, F. Huang and X. Yan, A Self-Cross-Linking Supramolecular Polymer Network Enabled by Crown-Ether-Based Molecular Recognition, *J. Am. Chem. Soc.*, 2020, **142**, 2051–2058.
7 (a) R. P. Sijbesma, F. H. Beijer, L. Brunsveld, B. J. B. Folmer, J. H. K. K. Hirschberg, R. F. M. Lange, J. K. L. Lowe and E. W. Meijer, Reversible Polymers Formed from Self-Complementary Monomers Using Quadruple Hydrogen Bonding, *Science*, 1997, **278**, 1601–1604; (b) B. J. B. Folmer, R. P. Sijbesma and E. W. Meijer, Unexpected Entropy-Driven Ring-Opening Polymerization in a Reversible Supramolecular System, *J. Am. Chem. Soc.*, 2001, **123**, 2093–2094; (c) V. Berl, M. Schmutz, M. J. Krische, R. G. Khoury and J.-M. Lehn, Supramolecular Polymers Generated from Heterocomplementary Monomers Linked through Multiple Hydrogen-Bonding Arrays—Formation, Characterization, and Properties, *Chem. Eur. J.*, 2002, **8**, 1227–1244.
8 (a) W. Weng, Z. Li, A. M. Jamieson and S. J. Rowan, Control of Gel Morphology and Properties of a Class of Metallo-Supramolecular Polymers by Good/Poor Solvent Environments, *Macromolecules*, 2009, **42**, 236–246; (b) T. Vermonden, M. J. van Steenbergen, N. A. M. Besseling, A. T. M. Marcelis, W. E. Hennink, E. J. R. Sudhölter and M. A. Cohen Stuart, Linear Rheology of Water-Soluble Reversible Neodymium(III) Coordination Polymers, *J. Am. Chem. Soc.*, 2004, **126**, 15802–15808.
9 (a) D. Ogata, T. Shikata and K. Hanabusa, Chiral Amplification of the Structure and Viscoelasticity of a Supramolecular Polymeric System Consisting of *N*,*N*',*N*''-Tris(3,7-

Open Access Article. Published on 14 April 2026. Downloaded on 4/15/2026 3:10:24 AM.
This article is licensed under a Creative Commons Attribution-NonCommercial 3.0 Unported Licence.
Chemical Science Accepted Manuscript

View Article Online
DOI: 10.1039/D5SC09763K

Dimethyloctyl)Benzene-1,3,5-Tricarboxamide and *n*-Decane, *J. Phys. Chem. B*, 2004, **108**, 15503–15510; (b) T. Shikata, D. Ogata and K. Hanabusa, Viscoelastic Behavior of Supramolecular Polymeric Systems Consisting of *N*,*N*',*N*''-Tris(3,7-dimethyloctyl)benzene-1,3,5-tricarboxamide and *n*-Alkanes, *J. Phys. Chem. B*, 2004, **108**, 508–514.

10 (a) P. Terech, V. Schaffhauser, P. Maldivi and J. M. Guenet, Living polymers in organic solvents, *Langmuir*, 1992, **8**, 2104–2106; (b) C. Dammer, P. Maldivi, P. Terech and J.-M. Guenet, Rheological Study of a Bicopper Tetracarboxylate/Decalin Jelly, *Langmuir*, 1995, **11**, 1500–1506; (c) G. Ducouret, C. Chassenieux, S. Martins, F. Lequeux and L. Bouteiller, Rheological characterisation of bis-urea based viscoelastic solutions in an apolar solvent, *J. Colloid Interface Sci.*, 2007, **310**, 624–629; (d) S. Seiffert and J. Sprakel, Physical chemistry of supramolecular polymer networks, *Chem. Soc. Rev.*, 2012, **41**, 909–930.

11 E. Vereroudakis, N. A. Burger, L. Bouteiller, B. Loppinet, E. W. Meijer, D. Vlassopoulos and N. J. Van Zee, Counterintuitive Viscoelasticity of Supramolecular Polymer Networks Driven by Coassembly with Water Molecules, *Macromolecules*, 2024, **57**, 9030–9040.

12 (a) N. M. Sangeetha and U. Maitra, Supramolecular gels: Functions and uses, *Chem. Soc. Rev.*, 2005, **34**, 821–836; (b) E. R. Draper and D. J. Adams, Low-Molecular-Weight Gels: The State of the Art, *Chem*, 2017, **3**, 390–410. (c) D. K. Smith, Supramolecular gels – a panorama of low-molecular-weight gelators from ancient origins to next-generation technologies, *Soft Matter*, 2024, **20**, 10–70.

13 (a) L. Chen, J. Raeburn, S. Sutton, D. G. Spiller, J. Williams, J. S. Sharp, P. C. Griffiths, R. K. Heenan, S. M. King, A. Paul, S. Furzeland, D. Atkins and D. J. Adams, Tuneable mechanical properties in low molecular weight gels, *Soft Matter*, 2011, **7**, 9721–9727; (b) W. E. M. Noteborn, D. N. H. Zwagerman, V. S. Talens, C. Maity, L. van der Mee, J. M. Poolman, S. Mytnyk, J. H. van Esch, A. Kros, R. Eelkema and R. E. Kieltyka, Crosslinker-Induced Effects on the Gelation Pathway of a Low Molecular Weight Hydrogel, *Adv. Mater.*, 2017, **29**, 1603769; (c) A. Dawn and H. Kumari, Low Molecular Weight Supramolecular Gels Under Shear: Rheology as the Tool for Elucidating Structure–Function Correlation, *Chem. Eur. J.*, 2018, **24**, 762–776; (d) R. Laishram, S. Sarkar, I. Seth, N. Khatun, V. K. Aswal, U. Maitra and S. J. George, Secondary Nucleation-Triggered Physical Cross-Links and Tunable Stiffness in Seeded Supramolecular Hydrogels, *J. Am. Chem. Soc.*, 2022, **144**, 11306–11315.

14 S. Liu, W. Yu and C. Zhou, Solvents effects in the formation and viscoelasticity of DBS organogels, *Soft Matter*, 2013, **9**, 864–874.

15 F. Lortie, S. Boileau, L. Bouteiller, C. Chassenieux, B. Demé, G. Ducouret, M. Jalabert, F. Lauprêtre and P. Terech, Structural and Rheological Study of a Bis-urea Based Reversible Polymer in an Apolar Solvent, *Langmuir*, 2002, **18**, 7218–7222.

16 S. Panja and D. J. Adams, Gel to gel transitions by dynamic self-assembly, *Chem. Commun.*, 2019, **55**, 10154–10157.

17 (a) K. J. Skilling, F. Citossi, T. D. Bradshaw, M. Ashford, B. Kellam and M. Marlow, Insights into low molecular mass organic gelators: a focus on drug delivery and tissue engineering applications, *Soft Matter*, 2014, **10**, 237–256; (b) B. O. Okesola and D. K. Smith, Applying low-molecular weight supramolecular gelators in an environmental setting – self-assembled gels as smart materials for pollutant removal, *Chem. Soc. Rev.*, 2016, **45**, 4226–4251; (c) T. Christoff-Tempesta, A. J. Lew and J. H. Ortony, Beyond Covalent Crosslinks: Applications of Supramolecular Gels. *Gels*, 2018, **4**, 40; (d) S. Panja and D. J. Adams, Stimuli responsive dynamic transformations in supramolecular gels, *Chem. Soc. Rev.*, 2021, **50**, 5165–5200; (e) D. K. Smith, Supramolecular Gels as Active Tools for Reaction Engineering, *Angew. Chem. Int. Ed.*, 2025, **64**, e202502053.

18 J. J. B. van der Tol, G. Vantomme and E. W. Meijer, Solvent-Induced Pathway Complexity of Supramolecular Polymerization Unveiled Using the Hansen Solubility Parameters, *J. Am. Chem. Soc.*, 2023, **145**, 17987–17994.

19 T. Shimada, Y. Watanabe, T. Kajitani, M. Takeuchi, Y. Wakayama and K. Sugiyasu, Individually separated supramolecular polymer chains toward solution-processable supramolecular polymeric materials, *Chem. Sci.*, 2023, **14**, 822–826.

20 (a) F. Wudl and G. Srdanov, Conducting polymer formed of poly(2-methoxy,5-(2'-ethyl-hexyloxy)-*p*-phenylenevinylene), *United States Patent 5*, 189, 136, 1993; (b) X. Zhan, Z. a. Tan, B. Domercq, Z. An, X. Zhang, S. Barlow, Y. Li, D. Zhu, B. Kippelen and S. R. Marder, A High-Mobility Electron-Transport Polymer with Broad Absorption and Its Use in Field-Effect Transistors and All-Polymer Solar Cells, *J. Am. Chem. Soc.*, 2007, **129**, 7246–7247; (c) I. Osaka, R. Zhang, J. Liu, D.-M. Smilgies, T. Kowalewski and R. D. McCullough, Highly Stable Semiconducting Polymers Based on Thiazolothiazole, *Chem. Mater.*, 2010, **22**, 4191–4196; (d) T. Lei, J.-H. Dou and J. Pei, Influence of Alkyl Chain Branching Positions on the Hole Mobilities of Polymer Thin-Film Transistors, *Adv. Mater.*, 2012, **24**, 6457–6461; (e) F. Zhang, Y. Hu, T. Schuettfort, C.-a. Di, X. Gao, C. R. McNeill, L. Thomsen, S. C. B. Mannsfeld, W. Yuan, H. Sirringhaus and D. Zhu, Critical Role of Alkyl Chain Branching of Organic Semiconductors in Enabling Solution-Processed N-Channel Organic Thin-Film Transistors with Mobility of up to 3.50 $cm^2 V^{-1} s^{-1}$, *J. Am. Chem. Soc.*, 2013, **135**, 2338–2349; (f) J. Mei and Z. Bao, Side Chain Engineering in Solution-Processable Conjugated Polymers, *Chem. Mater.*, 2014, **26**, 604–615; (g) K. Kawabata, M. Saito, N. Takemura, I. Osaka and K. Takimiya, Effects of branching position of alkyl side chains on ordering structure and charge transport property in thienothiophenedione- and quinacridone-based semiconducting polymers, *Polym. J.*, 2017, **49**, 169–176. (h) A. Shinohara, C. Pan, Z. Guo, L. Zhou, Z. Liu, L. Du, Z. Yan, F. J. Stadler, L. Wang and T. Nakanishi, Viscoelastic Conjugated Polymer Fluids, *Angew. Chem. Int. Ed.*, 2019, **58**, 9581–9585.

21 (a) Y. Yang, H. Qin, M. Jiang, L. Lin, T. Fu, X. Dai, Z. Zhang, Y. Niu, H. Cao, Y. Jin, F. Zhao and X. Peng, Entropic Ligands for Nanocrystals: From Unexpected Solution Properties to Outstanding Processability, *Nano Lett.*, 2016, **16**, 2133–2138; (b) O. Elimelech, O. Aviv, M. Oded, X. Peng, D. Harries and U. Banin, Entropy of Branching Out: Linear versus Branched Alkylthiols Ligands on CdSe Nanocrystals, *ACS Nano*, 2022, **16**, 4308–4321; (c) S. Yamashita, Y. Ito, H. Kamiya and Y. Okada, Surface coverage can control the dispersibility of TiO_2 and ZrO_2 nanoparticles in hydrophobic solvents: Comparison of linear and branched ligands, *Adv. Powder Technol.*, 2024, **35**, 104277.

22 (a) J. J. Armao IV, M. Maaloum, T. Ellis, G. Fuks, M. Rawiso, E. Moulin and N. Giuseppone, Healable Supramolecular Polymers as Organic Metals, *J. Am. Chem. Soc.*, 2014, **136**, 11382–11388; (b) E. Moulin, J. J. Armao IV and N. Giuseppone, Triarylamine-Based Supramolecular Polymers: Structures, Dynamics, and Functions, *Acc. Chem. Res.*, 2019, **52**, 975–983.

23 (a) K. Kubo, Y. Moriyama, S. Ujiie and A. Mori, Synthesis and Properties of New Liquid Crystalline Organogelators with a Tris[4-(benzoylamino)phenyl]amine Core, *Chem. Lett.*, 2015, **44**, 984–986; (b) T. Kim, T. Mori, T. Aida and D. Miyajima, Dynamic propeller conformation for the unprecedentedly high degree of chiral amplification of supramolecular helices, *Chem. Sci.*, 2016, **7**, 6689–6694.

24 (a) J. J. van Gorp, J. A. J. M. Vekemans and E. W. Meijer, C3-Symmetrical Supramolecular Architectures: Fibers and Organic Gels from Discotic Trisamides and Trisureas, *J. Am.*

Open Access Article. Published on 14 April 2026. Downloaded on 4/15/2026 3:10:24 AM. This article is licensed under a Creative Commons Attribution-NonCommercial 3.0 Unported Licence.

Chemical Science Accepted Manuscript

View Article Online
DOI: 10.1039/D5SC09763K

Open Access Article. Published on 14 April 2026. Downloaded on 4/15/2026 3:10:24 AM.
This article is licensed under a Creative Commons Attribution-NonCommercial 3.0 Unported Licence.

Chem. Soc., 2002, **124**, 14759–14769; (b) M. Ikeda, M. Takeuchi and S. Shinkai, Unusual emission properties of a triphenylene-based organogel system, *Chem. Commun.*, 2003, 1354–1355; (c) M. Shirakawa, S. Kawano, N. Fujita, K. Sada and S. Shinkai, Hydrogen-Bond-Assisted Control of H versus J Aggregation Mode of Porphyrins Stacks in an Organogel System, *J. Org. Chem.*, 2003, **68**, 5037–5044; (d) T. Kishida, N. Fujita, K. Sada and S. Shinkai, Sol−Gel Reaction of Porphyrin-Based Superstructures in the Organogel Phase: Creation of Mechanically Reinforced Porphyrin Hybrids, *J. Am. Chem. Soc.*, 2005, **127**, 7298–7299.

25 (a) Y. Kudo, M. Sakuragi, S. Hashida, R. Kuwahara, T. Ishi-I, H. Masunaga and K. Sakurai, Flexibility and local structure of a worm-like cylinder of self-assembled discotic triazine triamide, *Polym. J.*, 2010, **42**, 812–817; (b) D. McDowall, D. J. Adams and A. M. Seddon, Using small angle scattering to understand low molecular weight gels, *Soft Matter*, 2022, **18**, 1577–1590.

26 H. M. M. ten Eikelder, A. J. Markvoort, T. F. A. de Greef and P. A. J. Hilbers, An Equilibrium Model for Chiral Amplification in Supramolecular Polymers, *J. Phys. Chem. B*, 2012, **116**, 5291–5301.

27 (a) P. Jonkheijm, P. van der Schoot, A. P. H. J. Schenning and E. W. Meijer, Probing the Solvent-Assisted Nucleation Pathway in Chemical Self-Assembly, *Science*, 2006, **313**, 80–83; (b) M. M. J. Smulders, A. P. H. J. Schenning and E. W. Meijer, Insight into the Mechanisms of Cooperative Self-Assembly: The "Sergeants-and-Soldiers" Principle of Chiral and Achiral C3-Symmetrical Discotic Triamides, *J. Am. Chem. Soc.*, 2008, **130**, 606–611.

28 (a) L. A. Holmes, S. Kusamizu, K. Osaki and J. D. Ferry, Dynamic mechanical properties of moderately concentrated polystyrene solutions, *J. Polym. Sci., Part A-2: Polym. Phys.*, 1971, **9**, 2009–2021; (b) V. R. Raju, E. V. Menezes, G. Marin, W. W. Graessley and L. J. Fetters, Concentration and molecular weight dependence of viscoelastic properties in linear and star polymers, *Macromolecules*, 1981, **14**, 1668–1676.

29 M. Doi, S. F. Edwards and S. F. Edwards, *The Theory of Polymer Dynamics*, Clarendon Press, 1988.

30 (a) D. C. Morse, Viscoelasticity of Concentrated Isotropic Solutions of Semiflexible Polymers. 2. Linear Response, *Macromolecules*, 1998, **31**, 7044–7067; (b) D. C. Morse, Viscoelasticity of Concentrated Isotropic Solutions of Semiflexible Polymers. 1. Model and Stress Tensor, *Macromolecules*, 1998, **31**, 7030–7043; (c) V. Shankar, M. Pasquali and D. C. Morse, Theory of linear viscoelasticity of semiflexible rods in dilute solution, *J. Rheol.*, 2002, **46**, 1111–1154.

31 R. G. Ricarte and S. Shanbhag, A tutorial review of linear rheology for polymer chemists: basics and best practices for covalent adaptable networks, *Polym. Chem.*, 2024, **15**, 815–846.

32 (a) T. Masuda, Y. Ohta and S. Onogi, Rheological Properties of Anionic Polystyrenes. III. Characterization and Rheological Properties of Four-Branch Polystyrenes, *Macromolecules*, 1971, **4**, 763–768; (b) W. W. Graessley, T. Masuda, J. E. L. Roovers and N. Hadjichristidis, Rheological Properties of Linear and Branched Polyisoprene, *Macromolecules*, 1976, **9**, 127–141; (c) W. W. Graessley and J. Roovers, Melt Rheology of Four-Arm and Six-Arm Star Polystyrenes, *Macromolecules*, 1979, **12**, 959–965; (d) L. J. Fetters, A. D. Kiss, D. S. Pearson, G. F. Quack and F. J. Vitus, Rheological behavior of star-shaped polymers, *Macromolecules*, 1993, **26**, 647–654.

33 M. E. Cates, Reptation of living polymers: dynamics of entangled polymers in the presence of reversible chain-scission reactions, *Macromolecules*, 1987, **20**, 2289–2296.

Chemical Science Accepted Manuscript

View Article Online
DOI: 10.1039/D5SC09763K

The data supporting this study are provided in the ESI.

Open Access Article. Published on 14 April 2026. Downloaded on 4/15/2026 3:10:24 AM.
This article is licensed under a Creative Commons Attribution-NonCommercial 3.0 Unported Licence.

Chemical Science Accepted Manuscript